Quantum Semiclass. Opt. **9** (1997) 785–796. Printed in the UK PII: S1355-5111(97)81696-X

Coexisting periodic attractors in injection-locked diode lasers

A Gavrielides†, V Kovanis†, P M Varangis†, T Erneux‡ and G Lythe‡§

† Nonlinear Optics Center, Phillips Laboratory, Kirtland AFB, NM 87117-5776, USA
‡ Université Libre de Bruxelles, Optique Nonlinéaire Théorique, Campus Plaine, CP 231, 1050 Bruxelles, Belgium

Received 3 February 1997, in final form 4 April 1997

Abstract. We present experimental evidence of coexisting periodic attractors in a semiconductor laser subject to external optical injection. The coexisting attractors appear after the semiconductor laser has undergone a Hopf bifurcation from the locked steady state. We consider the single-mode rate equations and derive a third-order differential equation for the phase of the laser field. We then analyse the bifurcation diagram of the time-periodic states in terms of the frequency detuning and the injection rate and show the existence of multiple periodic attractors.

1. Introduction

Semiconductor lasers have a wide range of applications because they are of relatively small size, they can be mass-produced at low cost and they are easy to operate. Applications of semiconductor lasers appear in many areas such as optical communication and high-speed modulation and detection. Despite their successful technology, semiconductor lasers are quite sensitive to any external perturbation which may destabilize their normal output. A small amount of optical feedback resulting from the reflection from an optical disc or from the end of an optical fibre is sufficient to generate pulsating instabilities. These oscillations are typically accompanied by higher intensity frequency noise and affect the normal efficiency of the laser.

Systematic experimental studies of semiconductor lasers, in particular, long-time series analyses of the intensity, are not available because the time scale of the intensity pulsations is typically in the picosecond regime. Fourier spectra measurements show a gradual increase of oscillatory instabilities as parameters are changed but do not reveal what the bifurcation mechanisms are. Most of the progress in our understanding of these bifurcations comes from extensive numerical studies of simple models and their comparison with the experimentally obtained Fourier spectra. Specifically, these are the Lang and Kobayashi equations [1] for a single-mode laser subject to optical feedback [2], the equations for two coupled lasers [3] and the equations for a laser subject to external optical injection [4]. The latter is presumably the simplest system which allows a study of instabilities induced by an external perturbation.

§ Present address: Center for Nonlinear Studies, Los Alamos National Laboratory, Los Alamos, NM 87545, USA.

1355-5111/97/050785+12$19.50

The rate equations in normalized form for this system consist of two equations for the complex electrical field E and the excess carrier number N given by

$$E' = (1 - \mathrm{i}b)NE + \eta E_i \tag{1}$$

$$TN' = P - N - P(1 + 2N)|E|^2 \tag{2}$$

where a prime denotes differentiation with respect to time t measured in units of the photon lifetime τ_p. The term $\eta E_i = \eta \exp(-\mathrm{i}\Omega t)$ models the electrical field of the injected signal which is controlled by changing either its amplitude η or its detuning Ω. The transformation from the standard semiconductor laser rate equations into equations (1) and (2) is described in the appendix of [5] (with $t = s, E = YP^{-1/2}\exp -(\mathrm{i}\Omega s), N = Z, b = -\alpha$ and $\eta = P^{-1/2}\mu$, where s, Y, Z, α and μ are the variables and parameters introduced in the appendix of [5]). Equations (1) and (2) are the same for a laser subject to optical feedback or for each laser in an array of coupled lasers. They differ only in the last term in equation (1). The fixed dimensionless parameters b, T and P are defined as follows: b is the linewidth enhancement factor ($b = 3$–6) which measures the amount of amplitude–phase coupling; $T \equiv \tau_s/\tau_p$ is the ratio of the carrier and photon lifetimes ($T \simeq 10^3$) and P is the dimensionless pumping current above threshold ($|P| < 1$). A series of recent experiments have explored a large variety of dynamical instabilities at high injection levels and have been simulated successfully by using equations (1) and (2). The comparison is particularly remarkable given the simplicity of these equations. They correctly describe the observed period-doubling cascade to chaos [6], the period-2 bubbles [7], as well as the details of the experimental map of all the instability regions in the detuning versus injection amplitude parameter space [8].

Of particular interest are the conditions for locking which corresponds to a steady phase of the laser field and occurs if the detuning is sufficiently low. This phenomenon is best analysed by introducing $E = R\exp[\mathrm{i}(\Phi - \Omega t)]$ into equations (1) and (2) and by studying the conditions for a steady phase Φ. If the injection level is very weak, it is reasonable to assume that the laser amplitude and the carrier number will approach their steady-state values in the absence of injection (i.e. $R \simeq 1$ and $N \simeq 0$) and that the long-time behaviour of the laser is first described by the phase Φ. From the equations for R, Φ and N, it is then straightforward to find that Φ satisfies Adler equation

$$\Phi' = \Omega - \eta \sin(\Phi)\,. \tag{3}$$

Locking now implies the condition $|\Omega| \leqslant \eta$. In addition to locking, equation (3) has been used to investigate the case of an unbounded phase (i.e. if $|\Omega| > \eta$). Specifically, if $\eta \ll \Omega$, $\Phi \simeq \Omega t$ which implies a small-amplitude periodic modulation of the laser amplitude equation, i.e. $R' = RN + \eta\cos(\Phi) \simeq RN + \eta\cos(\Omega t)$.

This case has been studied analytically [9] and is called four-wave mixing because of the typical Fourier spectra. However, the practical interest of equation (3) is limited by the fact that T is a large parameter. The effect of T large can be first analysed using equations (1) and (2) with $\eta = 0$. We find that small perturbations from the steady-state $(R, N) = (1, 0)$ slowly decays on an $\mathrm{O}(T)$ time interval with rapid oscillations characterized by period $2\pi/\omega = \mathrm{O}(\sqrt{T})$ where $\omega \equiv \sqrt{2P/T}$ is the laser relaxation oscillation frequency. We take this property into account by introducing the new time $s \equiv \omega t$ and by reformulating equations (1) and (2) in terms of normalized deviations from the steady state, namely, $x \equiv N\omega^{-1}$ and $y \equiv R - 1$. By then investigating the limit $\omega \to 0$ (equivalently, T large) of the resulting equations for x, y and Φ, we reobtain equation (3) provided that $\Omega = \mathrm{O}(\eta)$ and

$$\eta \leqslant \omega^2 = \mathrm{O}(T^{-1})\,. \tag{4}$$

Thus, equation (3) is only valid for relatively low injection. It explains the locking phenomenon and the entrainment of the laser in the four-wave mixing regime but cannot lead to the multiple instabilities observed experimentally and numerically.

In particular, in figures 1(a) and (b) we show experimentally obtained spectra of a semiconductor laser subject to injection operating at very low detunings between the frequencies of the slave and master laser. The spectra were taken at constant injection and detuning. They show the characteristic sidebands at the relaxation oscillation frequency indicating that a Hopf bifurcation has taken place from the locked steady state. The laser exhibited the two spectra at various times. The transition from one spectrum to another was abrupt, suggesting strongly that the laser was visiting two different periodic states assisted by the intrinsic noise in the system. This implies that another stable periodic state may coexist with the Hopf bifurcation periodic state for the same values of the parameters. During the measurements, the injected laser was oscillating in the same longitudinal mode.

Figures 2(a) and (b) show spectra obtained from solving the single-mode rate equations (1) and (2) numerically. The parameters used for these simulations were $T = 1000, b = 4, P = 1.0, \eta = 0.002$ and $\Omega/\omega = 0.1$. These values of the parameters are

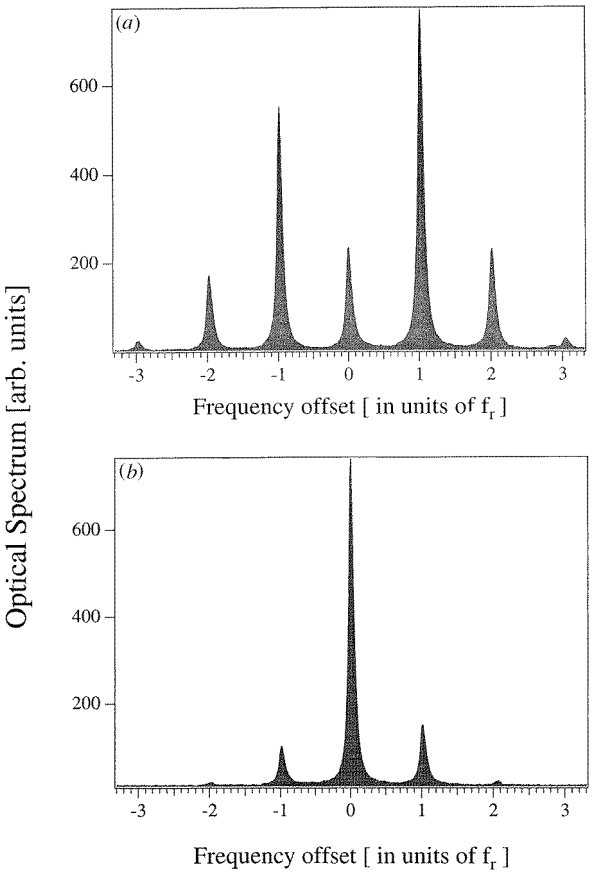

Figure 1. Experimentally obtained optical spectra of the laser subject to injection in the neighbourhood of the Hopf bifurcation. f_r is defined as the free-running relaxation oscillation frequency, $f_r = (1/2\pi)\sqrt{2P/T}$.

of the same order of magnitude as the values that have been used before by a number of authors to model the HLP-1400 semiconductor lasers (emitting at 830 nm). These lasers were also used in this set of experiments [10]. Gain saturation, known to shift bifurcation points, did not alter our conclusions, producing only minor modifications of the spectra. Figure 3 shows the bifurcation diagram of the periodic states. In addition to the periodic states emerging from the Hopf bifurcation, there is an isolated branch of periodic states emerging from a limit point. The spectra shown in figures 2(a) and (b) were computed at the points denoted by A and B in figure 3, respectively. They compare well with the experimental spectra shown in figures 1(a) and (b).

Bifurcation diagrams exhibiting coexisting bifurcation and isolated branches of periodic attractors are not common for nonlinear bifurcation problems. Similar diagrams have been found numerically for the laser subject to optical feedback [18] suggesting that the emergence of coexisting branches of periodic attractors is a general feature of semiconductor laser instabilities. This motivates analytical studies of the laser rate equations which we describe in the next two sections. In section 2, we formulate a third-order phase equation which is a

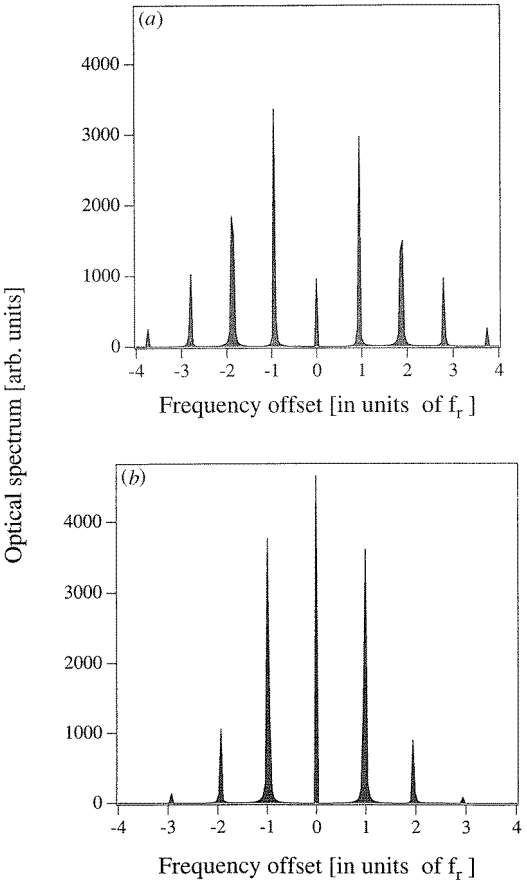

Figure 2. Numerically computed optical spectra from the single-mode rate equations (1) and (2) for $T = 1000, b = 4, P = 1.0, \eta = 0.002$ and $\Omega/\omega = 0.1$. The zero of the frequency scale denotes the frequency of the master laser.

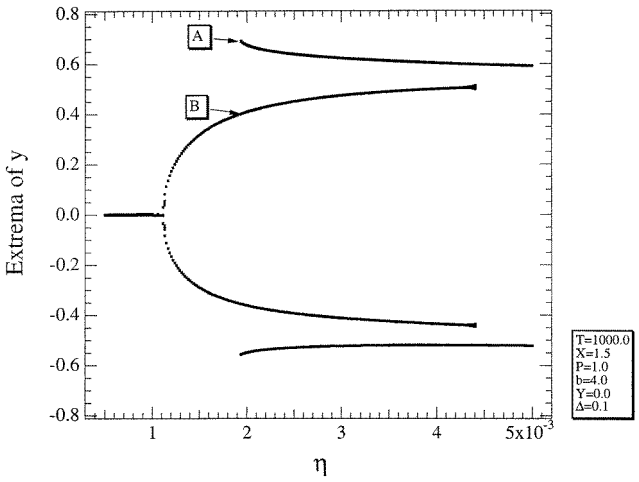

Figure 3. Bifurcation diagram of the extrema of the deviation of the field from steady state as a function of injection. The solutions are computed from the rate equations (1) and (2) using the same values of the parameters as in figure 2. The points denoted by A and B indicate where the spectra in figures 2(*a*) and (*b*) were computed numerically.

major simplification of the original laser equations. In section 3, we analyse this equation and determine approximations for the steady and time-periodic solutions.

2. Formulation

Intensive numerical studies of the first period-doubling bifurcation in the simplest case of zero detuning [11] showed that the linewidth enhancement factor plays a key role in the problem. Its relatively large value compared with the other constants in the problem explains why the intensity oscillations are nearly harmonic in time and how a strong coupling between phase and laser amplitude is possible. This can be demonstrated by a new asymptotic analysis of the original equations using b as the order parameter. To this end, we first introduce the decomposition $E = R\exp[\mathrm{i}(\Phi - \Omega t)]$ into equations (1) and (2) and reformulate the resulting three equations in terms of new variables defined by

$$s \equiv \omega t \qquad x \equiv Nb\omega^{-1} \qquad \text{and} \qquad y \equiv b(R-1)\,. \tag{5}$$

In equation (5), time is scaled by the relaxation oscillation frequency $\omega \equiv \sqrt{2P/T}$ and x, y represent deviations from the zero-injection steady-state solution $(R, N) = (1, 0)$. The resulting equations for x, y and Φ are then analysed for large b assuming $\omega = \mathrm{O}(b^{-1})$ (see the appendix). The reduced problem—accurate to $\mathrm{O}(b^{-1})$—is described in terms of the phase Φ and is given by equation (A10), or equivalently,

$$\Phi''' + (\xi - 2b^{-1}\Delta)\Phi'' + \Phi' - \Delta - \Lambda\cos(\Phi) = b^{-1}\left[\Lambda\sin(\Phi)\Phi'^{2} - \Lambda\sin(\Phi) - 2\Phi'\Phi''\right] \tag{6}$$

where a prime now denotes differentiation with respect to time s. The parameters Λ, Δ and ξ are defined by

$$\Lambda \equiv \frac{\eta b}{\omega} \qquad \Delta \equiv \frac{\Omega}{\omega} \qquad \text{and} \qquad \xi \equiv \omega\frac{1+2P}{2P} \tag{7}$$

and correspond to the normalized injection, normalized detuning and laser damping parameters, respectively. The leading-order problem as $b^{-1} \to 0$ (ω small but fixed) is

$$\Phi''' + \xi\Phi'' + \Phi' - \Delta - \Lambda\cos(\Phi) = 0 \tag{8}$$

and was examined previously for the case $\Delta = 0$ (zero detuning) [11]. In particular, its validity has been carefully investigated by comparing the numerical bifurcation diagrams obtained from equations (1) and (2) and from equation (8). The two bifurcation diagrams have been compared for various ranges of values of the parameters T and b including the experimental parameters estimated in [6–8]. The qualitative agreement between exact and approximate diagrams is excellent provided that the injection level is not too large ($0 < \Lambda < 1$). Quantitative agreement has been observed for $b = 10$. As b is decreased to $b = 4$, we note that the bifurcation branches of the rate equations (1) and (2) are smoother than the branches obtained from the reduced equation (8). A better agreement is expected if we use equation (6) instead of equation (8) since the first $O(b^{-1})$ correction terms have been taken into account in (6).

For the case $\Delta \neq 0$, a direct comparison between experimental data and the solutions of equation (8) has been undertaken if Δ is close to 2 and in the four-wave mixing region. If $\Delta \simeq 2$, the laser exhibits two period-doubling bifurcations which are not observed for other values of Δ and motivated the interest for this particular case. The optical spectra have been obtained for Δ below and above 2 which allow us to study both the sudden transition to subharmonic resonance and the progressive shift of the frequencies [12].

In this paper, we investigate equation (6). The steady states and their linear stability properties are easily determined for small b^{-1} and $\omega = O(b^{-1})$. We find that the steady states emerge from limit points located at

$$\Lambda = \Delta \tag{9}$$

and that they may change stability at Hopf bifurcation points located at

$$\Lambda = \sqrt{\Delta^2 + (\xi - 2b^{-1}\Delta)^2 + O(b^{-2})}\,. \tag{10}$$

From equations (9) and (10), we note that a limit point and a Hopf bifurcation point may coalesce if $\Delta = \Delta_c$ and $\Lambda = \Lambda_c$ where

$$\Delta_c \simeq \xi b/2 \qquad \text{and} \qquad \Lambda_c = \Delta_c\,. \tag{11}$$

This degenerate Hopf bifurcation point was already noticed from the exact linear stability analysis [13]. It corresponds to a zero eigenvalue and a pair of imaginary eigenvalues of the linearized theory and may lead to a secondary bifurcation to quasiperiodic oscillations [14].

3. Bifurcation equations

The phase equation (equation (8)) is a major simplification of the original laser equations. It models the laser problem as a weakly damped harmonic oscillator strongly driven by the phase of the laser field but it is still too complicated for exact solutions. In this section, we determine an asymptotic solution of equation (6) valid for small b^{-1}, Λ, Δ and ξ by the method of multiple scales [16]. To this end, we expand the parameters as

$$\begin{aligned} &\Lambda = b^{-1}(\lambda + b^{-1}\lambda_1 + \cdots) \qquad \Delta = b^{-1}(\delta + b^{-1}\delta_1 + \cdots) \\ &\xi \equiv \omega\frac{1+2P}{2P} = b^{-1}(\sigma + b^{-1}\sigma_1 + \cdots) \end{aligned} \tag{12}$$

and seek a solution of the form

$$\Phi(s, \tau, b^{-1}) = \Phi_0(s, \tau) + b^{-1}\Phi_1(s, \tau) + \cdots \tag{13}$$

where $\tau \equiv b^{-1}s$ is defined as a slow time variable. The fact that the solution depends on two independent time variables implies the chain rule $\Phi' = \Phi_s + b^{-1}\Phi_\tau$, where subscripts denote partial derivatives.

Inserting (12) and (13) into equation (6) and equating to zero the coefficients of each power of b^{-1} leads to a sequence of linear problems for the coefficients $\Phi_0, \Phi_1, \ldots$. Solving the equation for Φ_0 gives

$$\Phi = A\sin(s + v) + B + \mathrm{O}(b^{-1}) \tag{14}$$

where the amplitudes A and B and the phase v are functions of the slow time τ. We obtain equations for A, B and v by considering the problem for Φ_1 and by applying solvability conditions [16]. The equation for v is simply $v' = 0$ which means that v is equal to its initial value. The equations for A and B are given by

$$A' = -\tfrac{1}{2}\sigma A + \lambda\sin(B)J_1(A) \tag{15}$$

$$B' = \delta + \lambda\cos(B)J_0(A) \tag{16}$$

where $J_0(A)$ and $J_1(A)$ are Bessel functions which come from the expansion of $\cos(\Phi)$ in the Fourier series. Note that the modified phase equation (6) and the leading-order phase equation (8) lead to the same amplitude equations at this order of the analysis. Equations (15) and (16) admit steady-state solutions which we analyse in detail. The simplest solution is given by

$$\text{(i)} \qquad A = 0 \qquad \text{and} \qquad \Lambda = -\Delta\cos^{-1}(B) > 0 \tag{17}$$

and corresponds to the steady state of the original equation (8). The second steady-state solution of equations (15) and (16) is characterized by the fact that $A \neq 0$ and corresponds to time-periodic solutions of equation (8). It is instructive to examine this solution for $\Delta = 0$ first. From equation (16) with $B' = \delta = 0$, we find two possibilities. The first family of solutions verifies the condition $\cos(B) = 0$ and is described by

$$\text{(ii}a\text{)} \qquad B = \pm\frac{\pi}{2} \qquad \text{and} \qquad \Lambda = \pm\frac{\xi A}{2J_1(A)} > 0\,. \tag{18}$$

From equation (18), we determine a Hopf bifurcation branch emerging from solution (i) at $(\Lambda, A, B) = (\Lambda^H, 0, \pi/2)$. Λ^H is found from (18) by taking the limit $A \to 0$. We obtain

$$\Lambda^H = \xi \tag{19}$$

which correctly matches equation (10) if $\Delta = 0$. But equation (18) describes other branches of solutions. These branches of solutions are isolated and emerge from limit points that satisfy the condition $\Lambda'(A) = 0$. Using the second expression in (18), we find that these limit points are located at $(\Lambda, A, B) = (\Lambda^L, A^L, \pm\pi/2)$ where A^L and Λ^L satisfy the condition

$$J_2(A^L) = 0 \qquad \text{and} \qquad \Lambda^L = \pm\frac{\xi A^L}{2J_1(A^L)} > 0\,. \tag{20}$$

The second family of solutions characterized by an $A \neq 0$ verifies the condition $J_0(A) = 0$ and is described by

$$\text{(ii}b\text{)} \qquad J_0(A) = 0 \qquad \text{and} \qquad \Lambda = \frac{\xi A}{2\sin(B)J_1(A)} > 0\,. \tag{21}$$

This solution emerges from solution (ii*a*) at the pitchfork bifurcation point located at $(\Lambda, A, B) = (\Lambda^{PF}, A^{PF}, \pm\pi/2)$ where

$$J_0(A^{PF}) = 0 \qquad \text{and} \qquad \Lambda^{PF} = \pm\frac{\xi A^{PF}}{2J_1(A^{PF})} > 0\,. \tag{22}$$

In the case of nonzero detuning ($\Delta \neq 0$), we find that all $A \neq 0$ steady-state solutions of equations (15) and (16) are described by (in implicit form)

$$\Lambda = \left[\left(\frac{\Delta}{J_0(A)}\right)^2 + \left(\frac{\xi A}{2J_1(A)}\right)^2\right]^{1/2} \qquad \text{and} \qquad B = \arccos\left(-\frac{\Delta}{\Lambda J_0(A)}\right). \tag{23}$$

Equation (23) reveals several branches of solutions which converge to solutions (ii*a*) and (ii*b*) as $\Delta \to 0$. In figure 4, we show the bifurcation diagram of the solutions of equations (15) and (16) in terms of A versus Λ. The full and dotted curves correspond to $\Delta = 0$ and $\Delta = 0.01$, respectively. All stable and unstable branches of solutions have been drawn. Note the coexistence of multiple branches of solutions emerging from limit points. If $\Delta = 0$, these limits points correspond to simple roots of Bessel functions (see equations (20) and (22)).

The numerical bifurcation diagram of the stable solutions of equation (8) with $\Delta = 0$ is shown in figure 5. Figures 5(*a*) and (*b*) represent the extrema of the phase Φ and the intensity variable $y \equiv b(R-1)$, respectively. The pitchfork bifurcation at (22) leading to two distinct branches of B is clearly identified in figure 5(*a*). These two branches are not seen in figure 5(*b*) because $y = \Phi'' \simeq -A\sin(s+\upsilon)$ from (A8) and is independent of B, in the first approximation (equivalently, the extrema of y are equal to $\pm A$, in the first approximation). The figure shows one isolated branch of stable periodic states that coexist with the bifurcation branch. The bifurcation at $\Lambda \sim 0.65$ is a period-doubling bifurcation which is not predicted by equations (15) and (16) and which requires a different analysis [11].

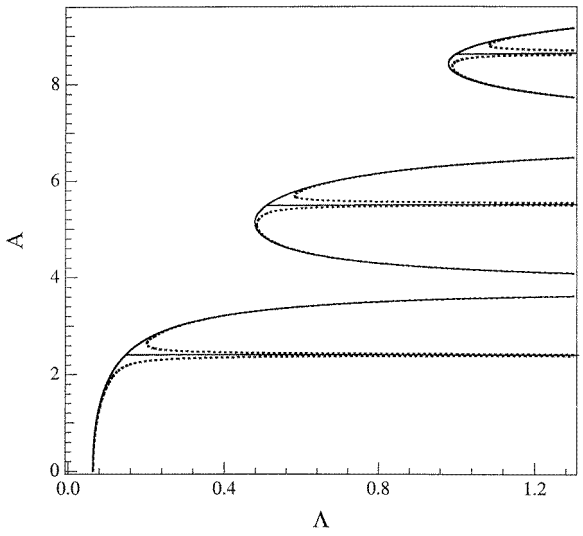

Figure 4. Bifurcation diagram of the amplitude A of the periodic solution versus Λ constructed from the analytic solutions of the phase equation for $T = 1000, b = 10, P = 0.5$. Full curves are for $\Delta = 0$ and dotted curves for $\Delta = 0.01$.

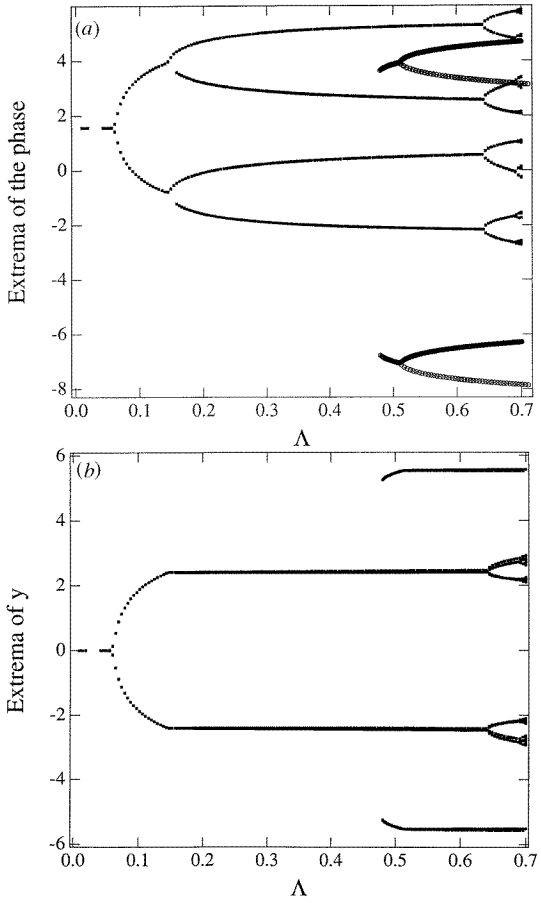

Figure 5. Bifurcation diagram obtained numerically from the phase equation (8) for $T = 1000, b = 10, P = 0.5$ and zero detuning. (*a*) Shows the extrema of the phase Φ versus injection Λ. (*b*) Shows the extrema of the field versus injection.

The unfolding of the $\Delta = 0$ bifurcation diagram as Δ is progressively increased is illustrated by the dotted curves in figure 4. In figure 6, we represent the extrema of y for all stable solutions determined numerically from (8) with $\Delta = 0.01$. The agreement between numerical and analytical solutions is excellent (compare figures 4 and 6).

The amplitude equations (15) and (16) admit a third family of solutions if $|\Delta/\Lambda| > 1$. These solutions correspond to $A = 0$ and an unbounded B satisfying Adler's equation, $B' = \Delta + \Lambda\cos(B)$. We have verified that all solutions of these equations are linearly stable with respect to small perturbations in A. Φ is then unbounded but Φ' is bounded (equivalently, $x \simeq \Delta - \Phi'$ and $y \simeq \Phi''$ are bounded). This solution is the four-wave solution for small Λ and $\Delta = \mathrm{O}(\Lambda)$.

In summary, our analysis of the phase equation (8) has revealed several branches of periodic solutions which allows the coexistence of different periodic states oscillating harmonically in time with similar periods but exhibiting differing amplitudes. Coexisting periodic states oscillating harmonically in time were also observed for the laser subject to optical feedback [18]. Both for the laser subject to injection and the laser subject to optical feedback, it is the strong phase–amplitude coupling parametrized by the

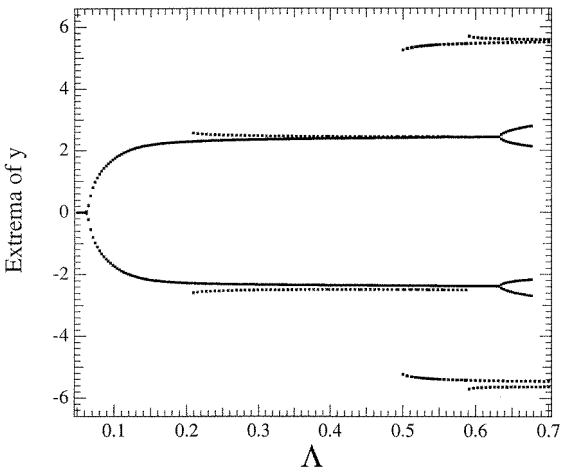

Figure 6. Bifurcation diagram obtained numerically from the phase equation (8) for $T = 1000$, $b = 10$, $P = 0.5$ and $\Delta = 0.01$.

linewidth enhancement factor b that is the main mechanism leading to this multiplicity of attractors.

Note that these periodic states appear as isolated branches of solutions. The traditional way to determine the bifurcation diagram of the long-time regimes is to follow each branch of solutions as a parameter is progressively changed and carefully determine changes of stabilities between each state. This method is used both experimentally and numerically but will fail to find isolated branches of solutions.

Isolated branches of solutions have been found numerically and experimentally for periodically modulated lasers [17]. These branches correspond to different resonances and coexisting periodic states admit different periods. In the case of a semiconductor laser subject to feedback, two periodic coexisting attractors were observed experimentally and computed numerically by Mork *et al* [2]. More recently, De Jagher *et al* [19] reported two coexisting periodic solutions which may result from the emergence of isolated branches of solutions as described in this paper. From a practical point of view, it could be interesting to force the semiconductor laser to operate at these higher intensity states and investigate possible application in communications or in logic gates.

4. Discussion

We have shown analytically that the single-mode equations admit multiple periodic states emerging from limit points in addition to periodic solutions that appear as the result of a Hopf bifurcation from the steady state. In general, the spectra of two of the limit cycles might appear to be very similar if they are taken at an injection level at which the amplitude saturates and approaches constant values. However, for low injection levels and away from saturation the spectra can exhibit dramatic differences. This is clearly demonstrated by the computed spectra shown in figure 2. In particular, small perturbations in the phase of the field can induce dramatic changes in the optical spectra. This is precisely the reason that the multiple instabilities exhibited by the phase of the field can be clearly observed in the spectra. Such effects include centre line suppression, in which the centre line of the laser is almost devoid of energy, most of which is carried by the sidebands at the

relaxation frequency. This is a typical feature of a laser with a large value of the linewidth enhancement factor.

The effect of gain saturation can also be incorporated in the context of the phase equation formalism. Its main contribution is to shift the Hopf bifurcation and limit points but it would not modify the qualitative properties of the bifurcation diagram.

We note that the period-doubling bifurcation point can also be captured analytically from equation (8) by seeking a solution of the form $\Phi \simeq A\sin(s) + D\cos(s/2)$. If $\Delta = 0$, we obtain

$$\Lambda_{PD} \simeq 0.62 \tag{24}$$

which compares well with the prediction of figure 5(a). If $\Delta \neq 0$, we find that the period-doubling bifurcation point $\Lambda_{PD}(\Delta)$ is, in parametric form, given by

$$\Lambda_{PD} = \frac{0.32}{J_1(A)} \qquad \Delta = \pm 0.32\frac{J_0(A)}{J_1(A)} \tag{25}$$

where $O(\xi)$ terms have been neglected.

The existence of sustained quasiperiodic oscillations has been suggested numerically, but requires a more detailed bifurcation analysis. Furthermore, experimental evidence of quasiperiodic oscillations is still lacking. This is partly because the laser is not stable in this injection region and mode hops frequently to a different cavity line. In addition, the transition to the quasiperiodic behaviour is a weak phenomenon and it is difficult to extract the signal from the background noise.

In conclusion, by taking advantage of the two large parameters T and b that are naturally present in semiconductor lasers, we are able to reduce the original single-mode rate equations into a third-order pendulum-type phase equation. This equation then allows us to predict isolated branching of solutions which cannot be anticipated using traditional continuation methods.

Acknowledgments

This research was supported by the US Air Force Office of Scientific Research grant AFOSR F49620-95-0065, The National Science Foundation grant DMS-9625843, NATO Collaborative Research Grant 961113, the Fonds National de la Recherche Scientifique (Belgium) and the InterUniversity Attraction Pole of the Belgian government.

Appendix. Derivation of the phase equation

We first introduce the decomposition $E = R\exp[\mathrm{i}(\Phi - \Omega t)]$ into equations (1) and (2) and obtain the following three equations for A, Φ and N:

$$R' = NR + \eta\cos(\Phi) \tag{A1}$$

$$\Phi' = \Omega - bN - \frac{\eta}{R}\sin(\Phi) \tag{A2}$$

$$TN' = P - N - P(1+2N)R^2\,. \tag{A3}$$

In equations (A1)–(A3), T is a large parameter that multiplies N'. We remove this source of singularity by introducing the new variables s, x and y defined by (5). Equations (A1)–(A3)

then become

$$y' = x(1 + b^{-1}y) + \Lambda\cos(\Phi) \tag{A4}$$

$$\Phi' = \Delta - x - \Lambda b^{-1}\frac{\sin(\Phi)}{1 + b^{-1}y} \tag{A5}$$

$$x' = -\xi x - y - 2\omega b^{-1}xy - \tfrac{1}{2}b^{-1}y^2 - \omega b^{-2}xy^2 \tag{A6}$$

where ξ, Λ and Δ are dimensionless parameters defined by (7). Note that ξ is proportional to ω and that ω is an $O(T^{-1/2})$ small quantity. Our problem depends on two small parameters, namely b^{-1} and ω. The derivation of our simplified problem will be based on the limit b^{-1} assuming $\omega = O(b^{-1})$.

From equations (A5), we find x as a function of Φ,

$$x = \Delta - \Phi' - \Lambda b^{-1}\sin(\Phi) + O(b^{-2}) \tag{A7}$$

and from equation (A6), using (A7), we find y as

$$y = -\xi x - x' + O(b^{-1}) = \Phi'' + O(b^{-1}, \omega)\,. \tag{A8}$$

(Note that the $O(b^{-1})$ correction term in (A7) is needed but the $O(b^{-1})$ and $O(\omega)$ correction terms in (A8) are not.) In order to derive an equation for Φ only, we first differentiate equation (A6) once and eliminate y' using equation (A4). We find

$$x'' = -\xi x' - \left[x(1 + b^{-1}y) + \Lambda\cos(\Phi)\right] - b^{-1}y\,(x + \Lambda\cos(\Phi)) + O(b^{-2}, b^{-1}\omega)\,. \tag{A9}$$

We next use (A7) and (A8) and eliminate x and y in equation (A9). This leads to the following third-order equation for Φ given by

$$\Phi''' + \Phi' - \Delta - \Lambda\cos(\Phi) + b^{-1}\left[\Phi''\left(b\xi - 2(\Delta - \Phi')\right) + \Lambda\sin(\Phi) - \Lambda\sin(\Phi)\Phi'^2\right] + O(b^{-2}, b^{-1}\omega) \tag{A10}$$

where $b\xi = O(b\omega)$ is $O(1)$.

References

[1] Lang R and Kobayashi K 1980 *IEEE J. Quantum Electron.* **QE-16** 347
[2] Mork J, Mark J and Tromborg B 1990 *Phys. Rev. Lett.* **65** 1999
[3] Winful H G and Wang S S 1988 *Appl. Phys. Lett.* **53** 1894
[4] Lang R 1982 *IEEE J. Quantum Electron.* **QE-18** 976
[5] Erneux T, Gavrielides A and Kovanis V Low pump stability of an optically injected diode laser *Quantum Semiclass. Opt.* **9** 811–8
[6] Simpson T B, Liu J M, Gavrielides A, Kovanis V and Alsing P M 1994 *Appl. Phys. Lett.* **64** 3539
[7] Simpson T B, Liu J M, Gavrielides A, Kovanis V and Alsing P M 1995 *Phys. Rev.* A **51** 4181
[8] Kovanis V, Gavrielides A, Simpson T B and Liu J M 1995 *Appl. Phys. Lett.* **67** 2780
[9] Lenstra D, van Tartwijk G H M, van der Graaf W A and de Jagher P C 1993 *SPIE* **2039** 11
[10] Li H, Ye J and McInerney J G 1993 *IEEE J. Quantum. Electron.* **QE-29** 2421
[11] Erneux T, Kovanis V, Gavrielides A and Alsing P M 1996 *Phys. Rev.* A **53** 4372
[12] Gavrielides A, Kovanis V, Varangis P M, Erneux T and Simpson T 1996 *SPIE* **3693** 654
[13] Gavrielides A, Kovanis V and Erneux T 1997 *Opt. Commun.* **136** 253
[14] Guckenheimer J and Holmes P 1983 *Nonlinear Oscillations, Dynamical Systems, and Bifurcations of Vector Fields* (*Applied Mathematical Sciences* **42**) (Berlin: Springer)
[15] Lee E K, Pang H S, Park J D and Lee H 1993 *Phys. Rev.* A **47** 736
[16] Kevorkian J and Cole J D 1981 *Perturbation Methods in Applied Mathematics (Applied Mathematical Sciences* **34**) (Berlin: Springer)
[17] Dangoisse D, Glorieux P and Hennequin D 1986 *Phys. Rev. Lett.* **57** 2657
Dangoisse D, Glorieux P and Hennequin D 1992 *Phys. Rev.* A **36** 4775
[18] Alsing P M, Kovanis V, Gavrielides A and Erneux T 1995 *Phys. Rev.* A **53** 4429
[19] De Jagher P C, van der Graaf W A and Lenstra D 1996 *Quantum Semiclass. Opt.* **8** 805